NASA TECHNICAL NOTE

NASA TN D-4383

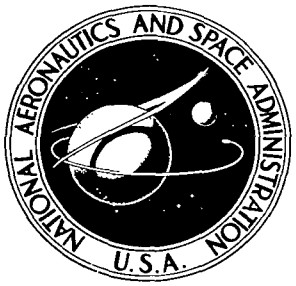

NASA TN D-4383

PERFORMANCE IN AIR OF 4-INCH- (10.16-CM-) MEAN-DIAMETER SINGLE-STAGE AXIAL-FLOW TURBINE FOR REYNOLDS NUMBERS FROM 4900 TO 188 000

by Hugh A. Klassen and Robert Y. Wong

Lewis Research Center
Cleveland, Ohio

NATIONAL AERONAUTICS AND SPACE ADMINISTRATION • WASHINGTON, D. C. • FEBRUARY 1968

PERFORMANCE IN AIR OF 4-INCH-(10.16-CM-) MEAN-DIAMETER SINGLE-STAGE AXIAL-FLOW TURBINE FOR REYNOLDS NUMBERS FROM 4900 TO 188 000

By Hugh A. Klassen and Robert Y. Wong

Lewis Research Center
Cleveland, Ohio

NATIONAL AERONAUTICS AND SPACE ADMINISTRATION

For sale by the Clearinghouse for Federal Scientific and Technical Information
Springfield, Virginia 22151 – CFSTI price $3.00

PERFORMANCE IN AIR OF 4-INCH- (10.16-CM-) MEAN-DIAMETER SINGLE-STAGE AXIAL-FLOW TURBINE FOR REYNOLDS NUMBERS FROM 4900 TO 188 000

by Hugh A. Klassen and Robert Y. Wong

Lewis Research Center

SUMMARY

A 4-inch- (10.16-cm-) mean-diameter turbine was investigated in air over a range of absolute inlet total pressures from 1.0 to 35.0 psia (0.69 to 24.13 N/cm^2) which corresponds to a Reynolds number range of 4900 to 188 000. Results were compared with those obtained for a reference 4-inch- (10.16-cm-) mean-diameter turbine with higher peak suction surface velocities on the stator and rotor and with higher rotor surface diffusion.

Peak efficiency for the subject turbine increased from 0.40 at the lowest Reynolds number to 0.63 at the highest. The turbine had higher peak efficiencies than the reference turbine over the entire Reynolds number range.

Stator- and rotor-outlet flow separation reported for the reference turbine was absent in the subject turbine except for the lowest Reynolds number of 4900, where the rotor-relative-outlet flow angle was 14° greater than design.

Rotor losses were smaller than those used in the turbine design. The stator overexpansion caused by these low losses resulted in negative rotor reaction.

Stator, rotor, and exit losses were computed for a blade-jet speed ratio of 0.32 and an overall static- to static-pressure ratio of 2.5. Losses were expressed as a fraction of ideal enthalpy. Stator losses decreased with increasing Reynolds number. Rotor losses decreased with increasing Reynolds number below a value of 15 000 and then remained almost constant. Exit losses were almost constant.

INTRODUCTION

Recent studies of the effect of Reynolds number on turbine performance have shown that performance varies little until low pressure levels are used. One such investigation (ref. 1) covered a Reynolds number range of 9400 to 144 000. In reference 1, turbine

efficiency decreased rapidly as the inlet total pressure was decreased below approximately 13 psia (9.0 N/cm^2). Below this pressure, operation became unstable. With turbine overall total- to static-pressure ratio and blade-jet speed ratio held constant, three separate curves were obtained for the variation of static efficiency with inlet total pressure. Also, as inlet total pressure was reduced below approximately 8.8 psia (6.1 N/cm^2), rotor losses increased faster than stator losses. Since stator reaction tended to minimize losses in reference 1, reaction in the rotor might also be expected to minimize rotor losses and depress the onset of unstable operation.

A 4-inch- (10.16-cm-) mean-diameter single-stage turbine was designed for the same equivalent weight flow as the turbine in reference 1 and the effect of rotor reaction on turbine performance was determined as Reynolds number was varied. The subject turbine was designed to operate at a Reynolds number of 14 390 with a stator discharge coefficient of 0.888, a reaction of 0.257, and an overall total efficiency of 0.500.

The design and the experimental results are presented herein with an analysis of the rotor and stator losses as computed from stator and rotor discharge coefficients.

TURBINE DESIGN

Design Conditions

The subject turbine was designed to have a mean diameter of 4 inches (10.16 cm) and a blade height of 0.125 inch (0.3175 cm). These dimensions are identical to those of the turbine of reference 1. In addition, the following design conditions were specified (see appendix A for symbol definition):

Equivalent weight flow, $W\sqrt{\theta_{cr}}\epsilon/\delta$, lb/sec; kg/sec	0.1436; 0.06514
Reynolds number, Re	14 390
Blade-jet speed ratio, ν	0.338
Inlet absolute total pressure, p_2', psia; N/cm^2	2.947; 2.032
Equivalent mean-section blade velocity, $U_m/\sqrt{\theta_{cr}}$, ft/sec; m/sec	400; 121.9
Equivalent specific work output, $\Delta h/\theta_{cr}$, Btu/lb; joules/g	12.78; 29.75
Total to total efficiency, η_t	0.500
Total pressure ratio across stator, p_3'/p_2'	0.888
Relative total pressure ratio across rotor, p_4''/p_3''	0.736
Reaction across rotor, R	0.257

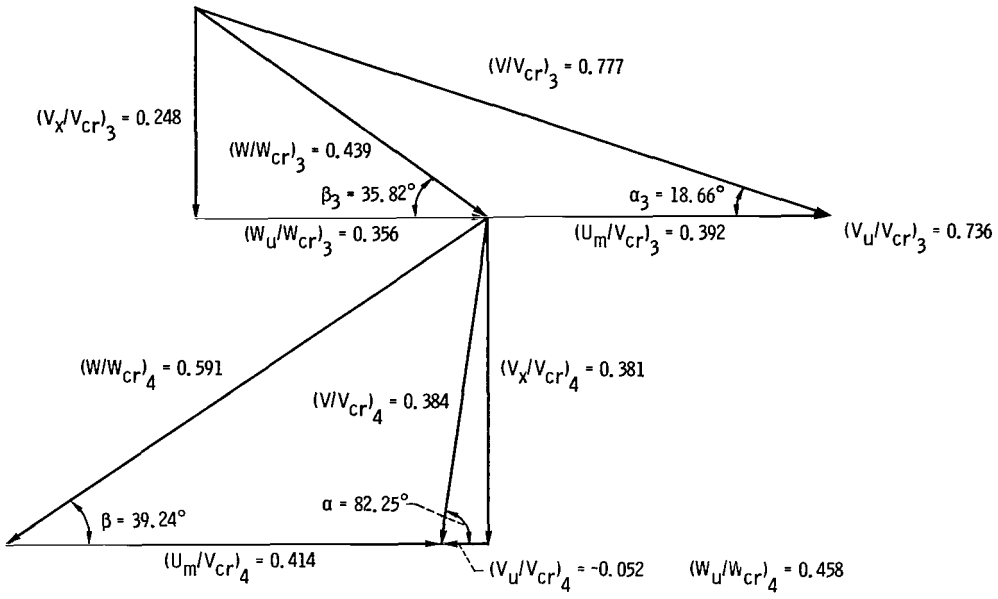

Figure 1. - Design velocity diagrams.

The design free-stream velocity diagrams consistent with these conditions are shown in figure 1.

The stator-outlet critical velocity ratio $(V/V_{cr})_3$ is 0.777. The stator-outlet discharge angle α_3 is 18.66°. The rotor-inlet relative critical velocity ratio $(W/W_{cr})_3$ is 0.439 and the relative rotor entrance angle is 35.82°. The rotor-outlet relative critical velocity ratio $(W/W_{cr})_4$ is 0.591, and the rotor has a relative discharge angle of 39.24°. Exit whirl is slightly negative, with an absolute tangential velocity ratio $(V_u/V_{cr})_4$ of 0.052 and an absolute exit flow angle α_4 of 82.25°.

Blade Design

The mean-section blade profiles for both the stator and the rotor were designed by an iterative process wherein a blade shape was assumed and surface velocity calculations were made by the method of reference 2 to match both continuity and the assumed loss distributions. Blade shapes were varied until the desired velocity distributions were obtained. In the analysis, the blade profile was assumed to be constant from hub to tip, and the total pressure loss was assumed to vary linearly from blade entrance to exit.

Stator description. - The design mean-section blade profiles, forming the flow channel for the stator, are shown in figure 2. The design mean-section surface velocity distribution for the channel, presented in figure 3(a), shows that the channel is a zero-diffusion suction surface design. The stator as constructed varied somewhat from design;

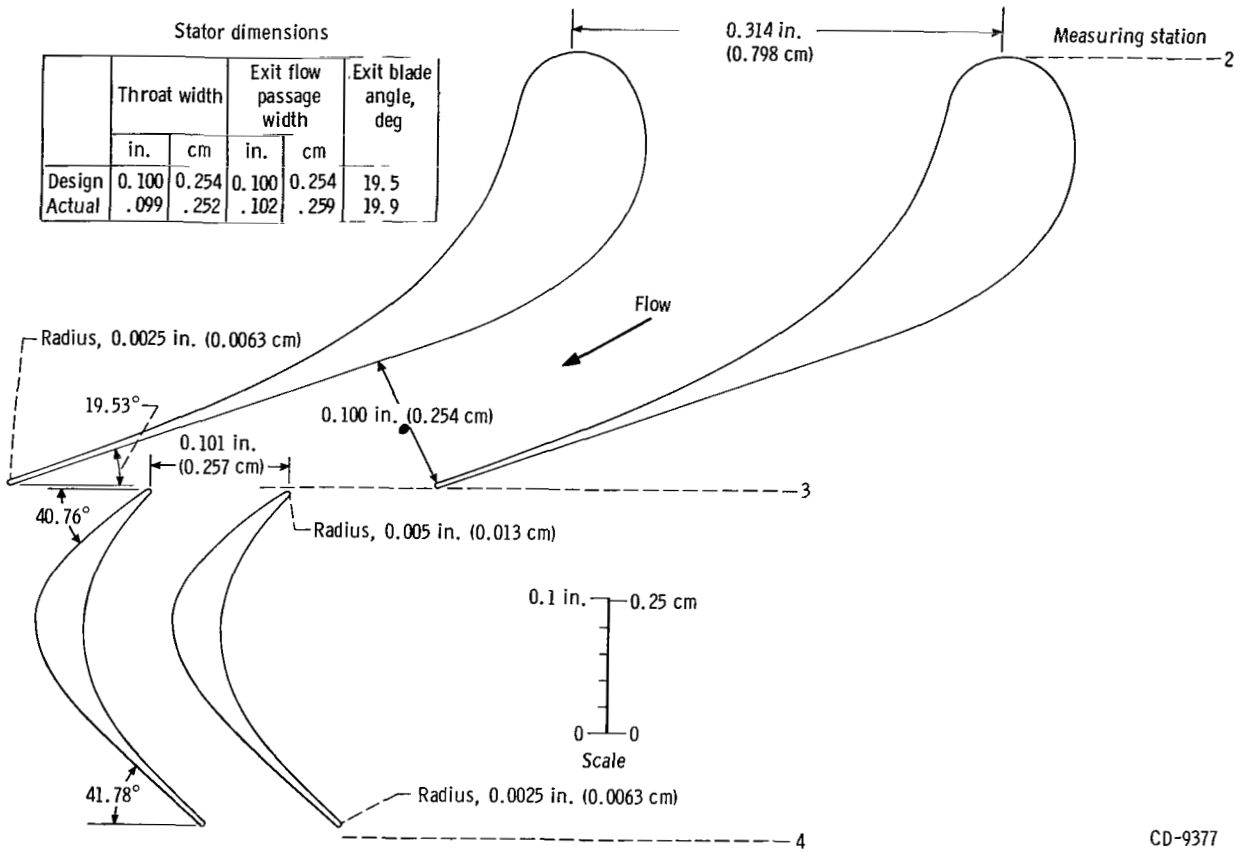

Figure 2. - Turbine design mean-section blade geometry.

the table presented in figure 2 compares the critical dimensions. The throat is 0.001 inch (0.0025 cm) less than design, which indicates that the stator throat area is about 1 percent lower than design. Further, the throat is not located at the channel exit, which results in a slight divergence in area from the throat to the channel exit. The design stator-blade coordinates are shown in table I. The 40 stator blades were furnace brazed to the inside and outside rings of the stator annulus.

Rotor description. - The design rotor-blade profiles forming the mean-section flow channel are presented in figure 2. The computed surface velocity distribution for this channel is presented in figure 3(b). The suction surface velocity rises to a maximum relative critical velocity ratio of 0.653 before it diffuses to the outlet relative critical velocity ratio of 0.604. A suction surface diffusion D_s of 0.075 results. The pressure surface velocity decreases from the relative inlet velocity ratio of 0.470 at the inlet to a minimum value of 0.310 before accelerating to the exit velocity. This amount of inlet deceleration gives a pressure surface diffusion D_p of 0.340 and a total diffusion D_t of 0.415. This value is approximately the maximum for good design practice. Higher values of total diffusion cause sharp increases in losses (ref. 3).

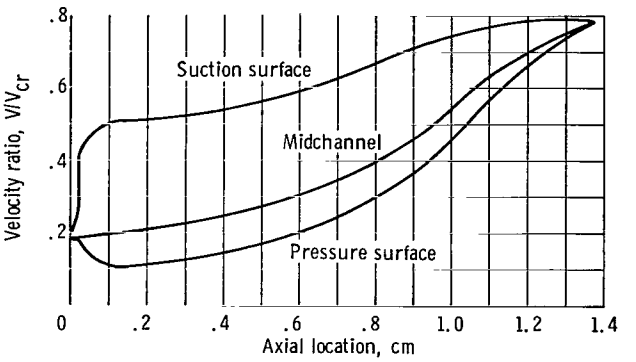

(a) Stator.

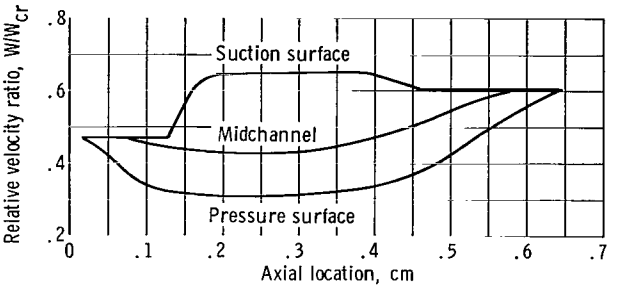

(b) Rotor.

Figure 3. - Design mean-section rotor and stator velocity distributions as functions of axial location.

The design rotor-blade coordinates are presented in table II. The 0.005-inch (0.0127-cm) tip clearance is the same as for the reference turbine. The 0.125-inch (0.3175-cm) rotor blades were fabricated by end milling the rotor disk.

APPARATUS, INSTRUMENTATION, AND PROCEDURE

The following apparatus was used in this investigation: the turbine; an airbrake to absorb and measure the power output of the turbine; air supplies for the turbine, the bearings, and the airbrake; and an exhaust system. A schematic diagram of the facility, showing these components, is presented in figure 4. Dry pressurized air was supplied to the turbine inlet through a pressure control valve. Weight flow was measured by a venturi operating under choked conditions. Turbine-exit flow passed through a control valve to the laboratory exhaust system.

A cutaway view of the turbine test assembly is given in figure 5. The turbine bearings were gas lubricated in order to minimize friction torque. Each of the two journal bearings had a 360° solid journal with eight orifices. The two-way thrust bearing had 360° thrust disks. The stationary thrust disks had four recessed orifices. The airbrake is described in reference 1.

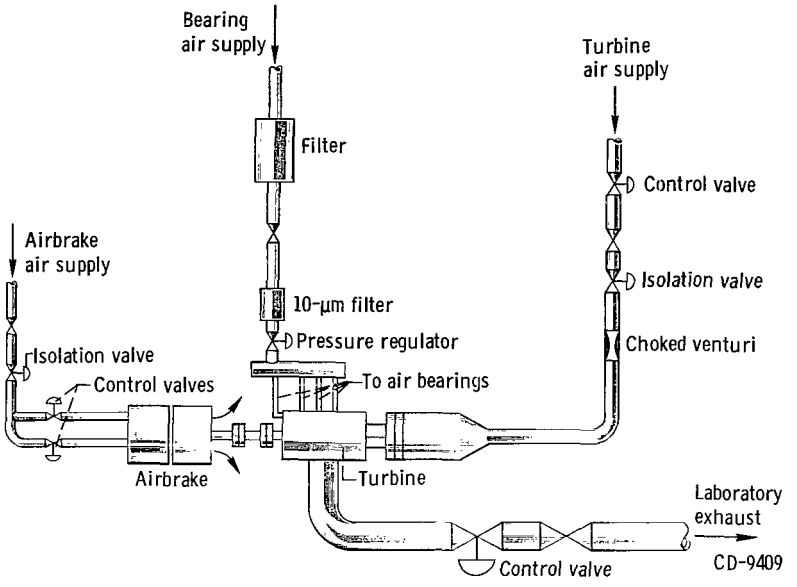

Figure 4. - Schematic diagram of test apparatus.

The turbine-inlet and turbine-outlet measuring stations are shown in figure 5. The measuring stations for the stator and rotor are shown in figure 2. Turbine-inlet total temperatures were measured by two thermocouples in the inlet collector (station 1). Stator-inlet static pressures were measured at station 2 (see fig. 2) with six taps, three at the inner wall (120° apart) and three at the outer wall (120° apart). Stator-inlet total pressure p_2' was calculated from measured static pressure, turbine-inlet temperature, weight flow, and annulus area. Stator-outlet static pressure p_3 was measured by three taps at the hub, located 120° apart. The stator has a negligible pressure difference between hub and tip because of the high hub-tip radius ratio and the constant design exit flow angle. Rotor-exit static pressures p_4 were measured with six taps, three at the hub (120° apart) and three at the tip (also 120° apart). Turbine-outlet static pressures p_5 were measured with two taps 180° apart in the outlet collector (see fig. 5).

Shaft torque was obtained with a commercial strain gage which measured the force applied by the airbrake torque arm. The equipment for measuring rotative speed consisted of a six-tooth sprocket mounted on the coupling, a proximity probe, and an electronic counter.

Turbine bearing and coupling windage losses were determined by removing the turbine rotor, driving the turbine shaft with the airbrake, and measuring the torque necessary to drive the turbine at various speeds. The friction torque was added to the torque measured during tests to obtain true turbine torque. The value of friction torque at design speed was 0.328 inch-pound (3.71 cm-N).

The experimental data were obtained by operating the turbine over a range of absolute inlet pressures from 1 to 35 psia (0.69 to 24.13 N/cm^2) at inlet-static to exit-static

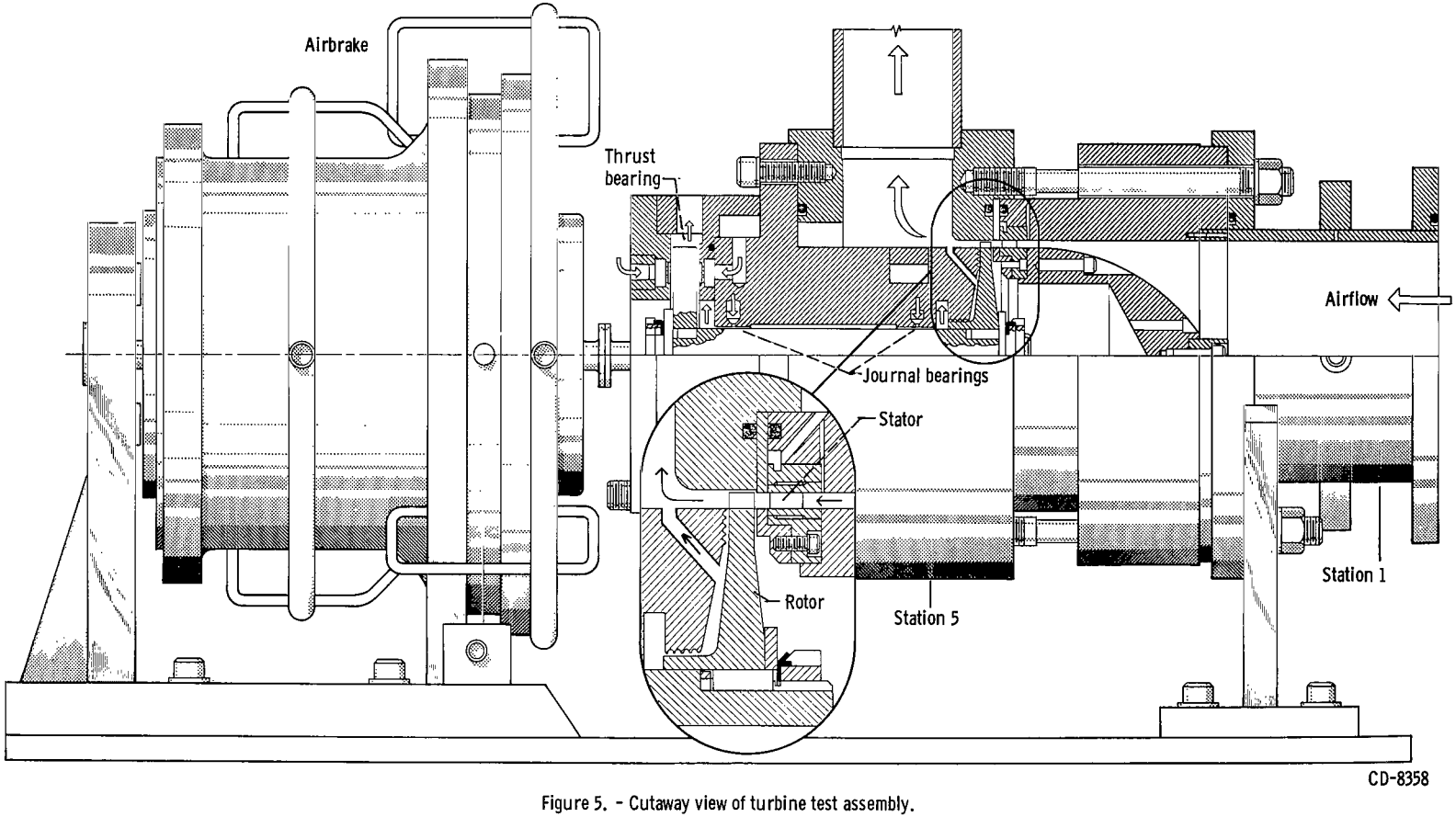

Figure 5. - Cutaway view of turbine test assembly.

pressure ratios of 2.0, 2.5, and 1.5 or 1.75. At each inlet pressure and pressure ratio, the turbine speed was varied from 5000 to 25 000 rpm in 2500-rpm increments. Inlet air temperature was approximately 535° R (297° K) for all tests.

RESULTS AND DISCUSSION

The results obtained when the subject 4-inch- (10.16-cm-) mean-diameter turbine was investigated over a range of absolute inlet total pressure from 1 to 35 psia (0.69 to 24.13 N/cm^2) are presented in terms of both overall turbine performance and stator and rotor performance. Comparison was made between the subject turbine and the turbine of reference 1 which had the same mean diameter and blade height, but different rotor surface velocity distributions.

The Reynolds number used in this report was used in reference 4 to correlate turbine loss data. When the stator is choked, this Reynolds number is constant for given inlet pressure and temperature. The values of inlet total pressure at which data were obtained and the corresponding Reynolds numbers for choked stator operation are given in the following table. At overall static- to static-pressure ratios below 2.5, some

Inlet total pressure		Reynolds number for choked stator, Re
psia	N/cm^2	
1	0.69	4 900
2	1.38	9 900
3	2.07	15 200
6	4.14	31 200
12	8.27	62 100
24	16.55	127 000
35	24.13	187 700

Reynolds numbers were lower than those shown in this table because the stator was not always choked. At each inlet total pressure, all Reynolds numbers were within 10 percent of those obtained with a choked stator.

The results are presented in two sections. The first section describes the overall performance of the turbine in terms of its torque and static efficiency characteristics over the range of Reynolds number covered. The second section then describes its performance at a blade-jet speed ratio of 0.32 and an overall static- to static-pressure ratio of 2.5, which correspond approximately to the design total- to static-pressure and blade-jet speed ratios. Included in this section are a description of weight flow and reaction characteristics of the turbine at this condition and the results of the velocity dia-

gram calculations that were made in accordance with the calculation procedure described in appendix B.

Overall Performance

The overall torque parameter characteristics of the subject turbine are presented in figure 6 as functions of blade-jet speed ratio ν and inlet total pressure p_2'. Data are presented on four separate curves (1) to isolate the effect of inlet pressure p_2', particularly at higher values of inlet pressure, and (2) to indicate the consistency of data for each inlet pressure.

It is shown in figure 6 that for any given blade-jet speed ratio, the torque parameter increased with increasing turbine-inlet pressure to a value of 24 psia (16.55 N/cm^2). No difference in torque parameter occurred when the turbine-inlet pressure was increased further to 35 psia (24.13 N/cm^2). Major differences occur in torque parameter with inlet pressures less than 6 psia (4.14 N/cm^2).

Turbine static efficiencies were computed from the torque parameter curves faired through the data in figure 6. The resulting efficiencies are presented in figure 7 as functions of blade-jet speed ratio ν and inlet total pressure p_2'. Peak static efficiency varied from about 0.40 at the lowest inlet pressure of 1.0 psia (0.69 N/cm^2) to 0.63 at an inlet total pressure of 35.0 psia (24.13 N/cm^2). This range of inlet pressure corresponds to a Reynolds-number range of 4900 to 188 000.

Figure 7 shows that the blade-jet speed ratio at which peak static efficiency occurred increased with increasing inlet total pressure to 24.0 psia (16.5 N/cm^2). The reasons for this trend can be described by introducing the velocity diagram parameter λ, which is defined as the ratio of the blade speed to the change in whirl velocity across the rotor. This speed-work parameter is also a function of static efficiency and blade-jet speed ratio $\lambda = 2\nu^2/\eta_s$. Peak static efficiencies for all inlet total pressures except 1.0 psia (0.69 N/cm^2) occurred at a speed-work parameter of approximately 0.64. This constant value indicates that the velocity diagrams for peak efficiency, at pressures of 2 psia (1.38 N/cm^2) and above, all have about the same shape. Peak efficiency for 1 psia (0.69 N/cm^2) occurred at a speed-work parameter of 0.56.

In figure 8, peak static efficiency is plotted against inlet total pressure for the subject and reference turbines. The subject-turbine peak static efficiency increased with increasing inlet total pressure to 24.0 psia (16.5 N/cm^2), which corresponds to a Reynolds number of 127 000. Above this pressure, peak static efficiency remained constant. The reference turbine peak static efficiency was constant above an inlet total pressure of 13.52 psia (9.33 N/cm^2), which corresponds to a Reynolds number of 70 000.

Peak efficiency for the subject turbine was appreciably higher than for the reference

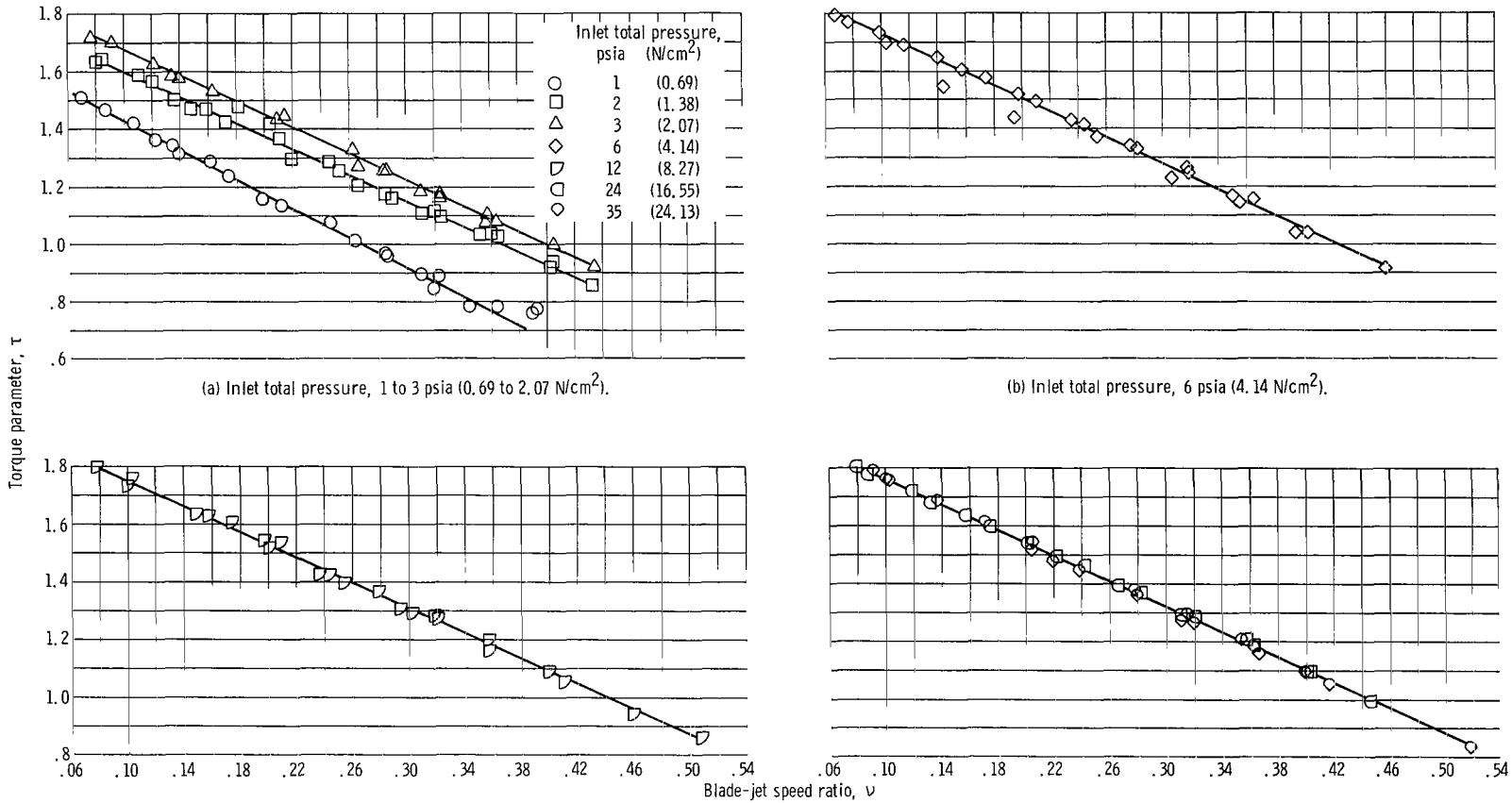

(a) Inlet total pressure, 1 to 3 psia (0.69 to 2.07 N/cm^2).

(b) Inlet total pressure, 6 psia (4.14 N/cm^2).

(c) Inlet total pressure, 12 psia (8.27 N/cm^2).

(d) Inlet total pressure, 24 and 35 psia (16.55 and 24.13 N/cm^2).

Figure 6. - Variation of torque parameter with inlet total pressure and blade-jet speed ratio.

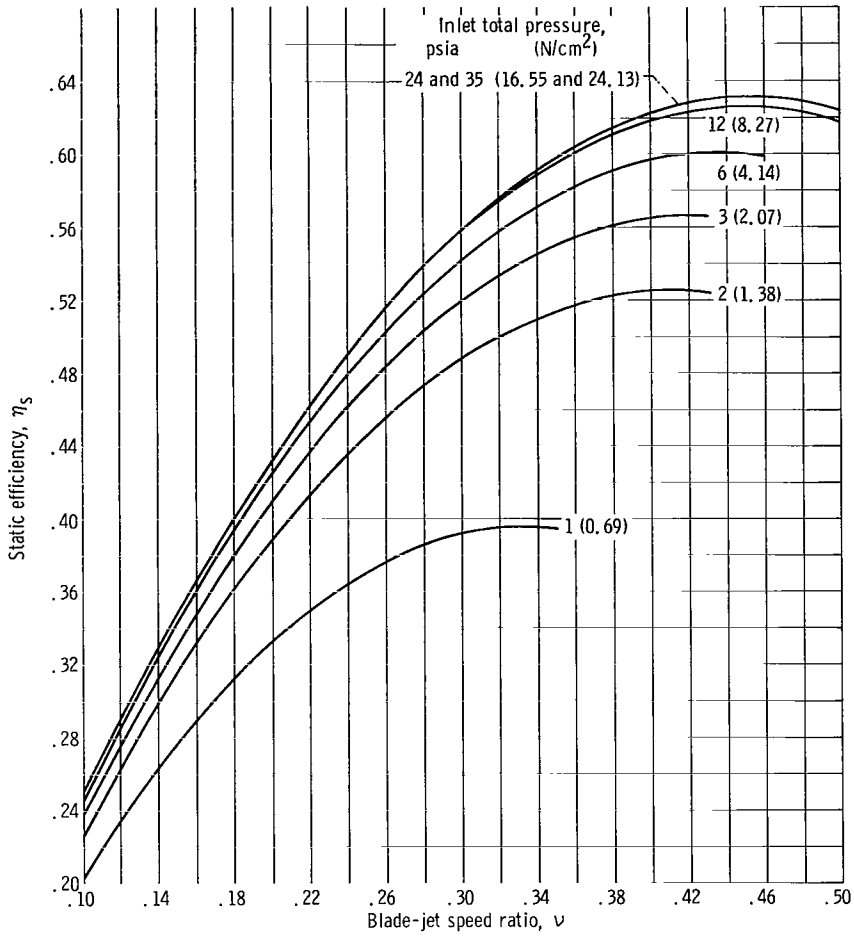

Figure 7. - Variation in static efficiency with inlet total pressure and blade-jet speed ratio.

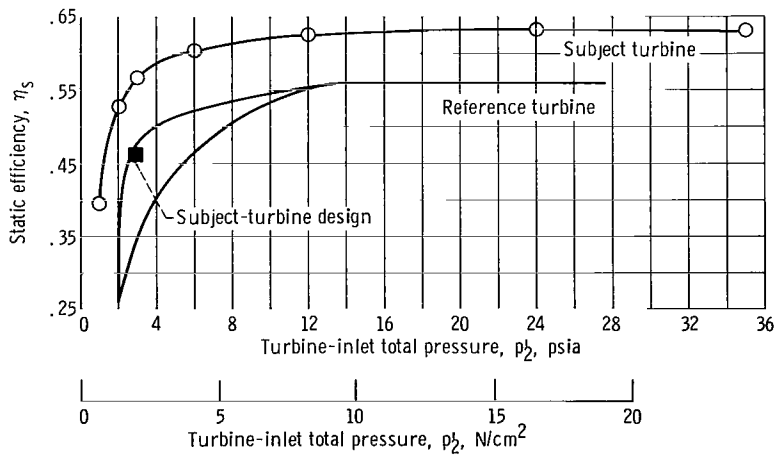

Figure 8. - Variation of peak static efficiency with inlet total pressure.

turbine at all pressures. At subject-turbine design inlet total pressure of 2.95 psia (2.03 N/cm^2), peak static efficiencies for the subject and reference turbines were 0.57 and 0.47, respectively. The reference turbine was tested over a range of inlet total pressures from 2.06 to 27.63 psia (1.42 to 19.05 N/cm^2) which corresponds to a Reynolds-number range of 9400 to 144 000 for the subject turbine. Peak static efficiencies for this pressure range varied from 0.53 to 0.63 for the subject turbine and from 0.26 to 0.56 for the reference turbine. This improved efficiency for the subject turbine results from lower rotor losses, which are discussed in the section Velocity diagram calculation results.

At design inlet total pressure, the actual static efficiency of 0.57 is 11 points higher than the design value of 0.46. For some inlet pressures, the reference turbine operated at either two or three efficiencies for a given blade-jet speed ratio because of the unstable operation mentioned in the INTRODUCTION. The double curve in figure 8 indicates the two highest efficiencies.

Performance at Blade-Jet Speed Ratio of 0.32 and Turbine Static- to Static-Pressure Ratio of 2.5

The performance of the subject turbine at given blade-jet speed ratio and pressure ratio is described herein to indicate the variation in the turbine behavior over the range of Reynolds number covered with these ratios remaining constant. The data used were obtained at a blade-jet speed ratio of 0.32 and a turbine inlet-static- to exit-static-pressure ratio of 2.5. These conditions were chosen because overall total- to static-pressure ratio and blade-jet speed ratio are close to design values at this condition. The weight flow and the pressure distributions obtained from the experimental data are described. Then the results of the velocity diagram calculations made under these conditions are presented, in addition to a description of the associated discharge coefficients and loss distribution (see appendix B for calculation method).

Weight flow and pressure distribution. - Figure 9 shows the effect of Reynolds number on equivalent weight flow. The equivalent weight flow varied 9 percent over a

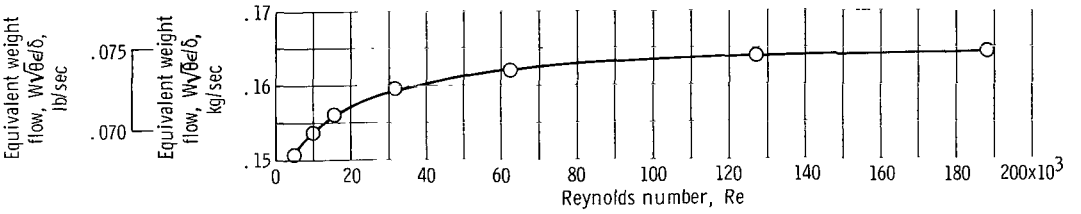

Figure 9. - Variation of turbine equivalent weight flow with Reynolds number. Turbine overall static- to static-pressure ratio, p_1/p_5, 2.5.

Reynolds number range of 4900 to 188 000. This variation was entirely the result of the change in stator discharge coefficient with Reynolds number, as is described in the section Velocity diagram calculation results. The stator was choked at all times at the overall pressure ratio of 2.5. Equivalent weight flow was, therefore, independent of changes in rotor losses.

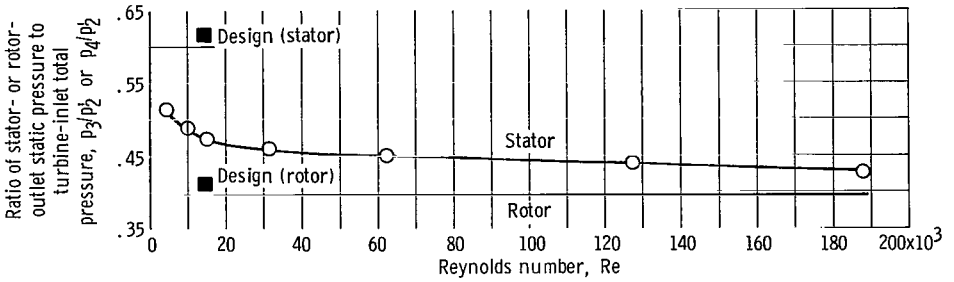

Figure 10. - Variation of stator- and rotor-outlet static pressures with Reynolds number. Blade-jet speed ratio, 0.32; turbine overall static- to static-pressure ratio, p_1/p_5, 2.5.

Figure 10 shows the variation in static pressure distribution with Reynolds number. Exit-static- to stator-inlet-total-pressure ratios p_3/p_2' and p_4/p_2' are plotted against Reynolds number for the stator and rotor. The rotor-exit- to stator-inlet-pressure ratio is constant because the turbine overall static pressure ratio p_1/p_5 was held constant at 2.5. The stator pressure ratio p_3/p_2' decreased with increasing pressure over the entire pressure range, which indicates a constantly decreasing rotor reaction. At the design Reynolds number of 14 400, p_3/p_2' is 0.472, while the design value is 0.61. This discrepancy between design and actual values results from rotor discharge coefficients being higher than design, as is described in the following section. The stator pressure ratio of 0.472, shown in figure 10 for design Reynolds number, indicates that the stator is choked and that stator-exit velocities are much higher than design.

Velocity diagram calculation results. - Free-stream velocity diagrams computed for the blade-jet speed ratio of 0.32 and an overall static- to static-pressure ratio of 2.5 are shown in figure 11 for the three lowest values of Reynolds number and for the highest. Comparison of these diagrams with design (fig. 1) shows that stator-exit velocities are much higher than design, which indicates rotor losses lower than design. The diagram for an inlet total pressure of 2.99 psia (2.07 N/cm^2), which is approximately the design value, show a slightly supersonic stator-exit velocity $(V/V_{cr})_3$ of 1.018 and a rotor-inlet relative velocity $(W/W_{cr})_3$ of 0.704. The corresponding design values are 0.777 for the stator and 0.439 for the rotor. Stator-exit velocity increased with increasing Reynolds number. The rotor-exit diagram at design inlet total pressure agrees approximately with the design diagram. The diagrams show that exit whirl is almost zero except for the lowest Reynolds number of 4940. Design whirl is slightly negative with an absolute tangential velocity ratio $(V_u/V_{cr})_4$ of -0.0517.

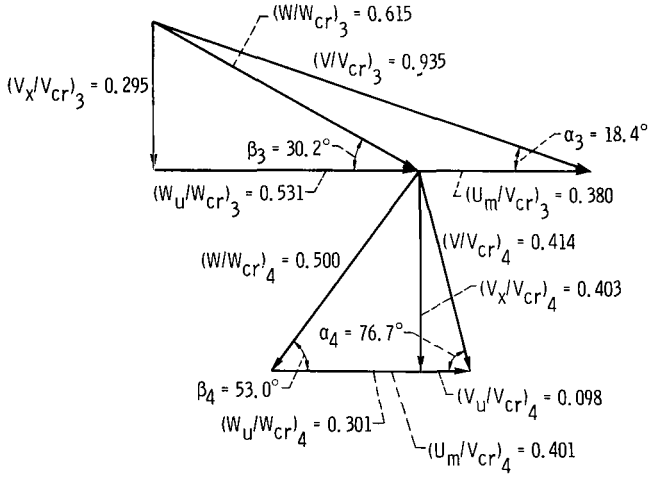

(a) Reynolds number, 4940; inlet total pressure, 1.006 psia (0.6936 N/cm^2).

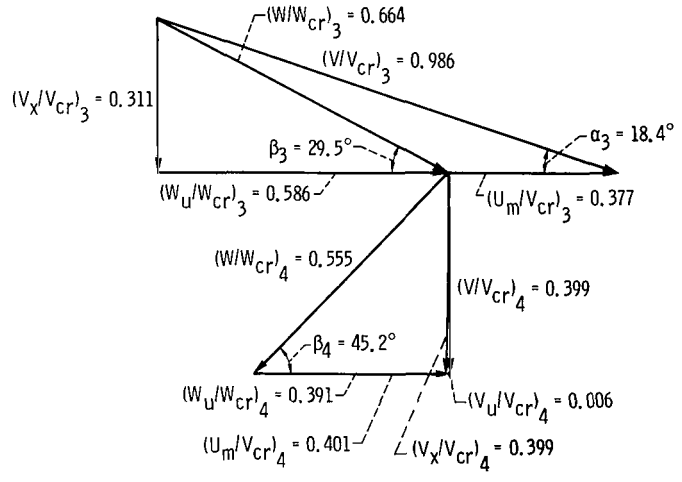

(b) Reynolds number, 9945; inlet total pressure, 1.990 psia (1.372 N/cm^2).

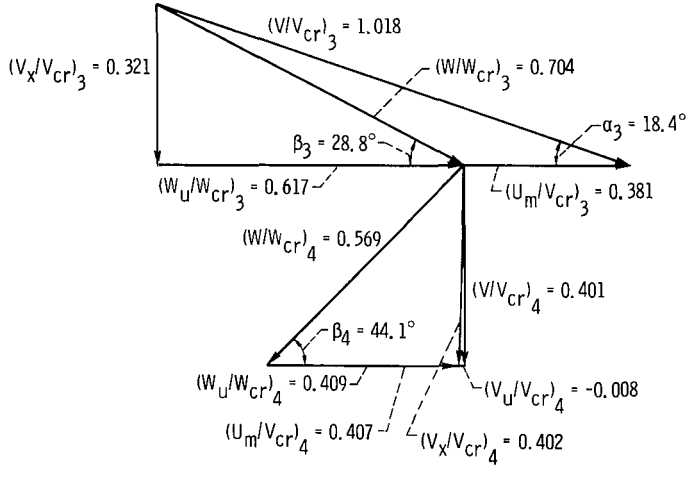

(c) Reynolds number, 15 170; inlet total pressure, 2.995 psia (2.065 N/cm^2).

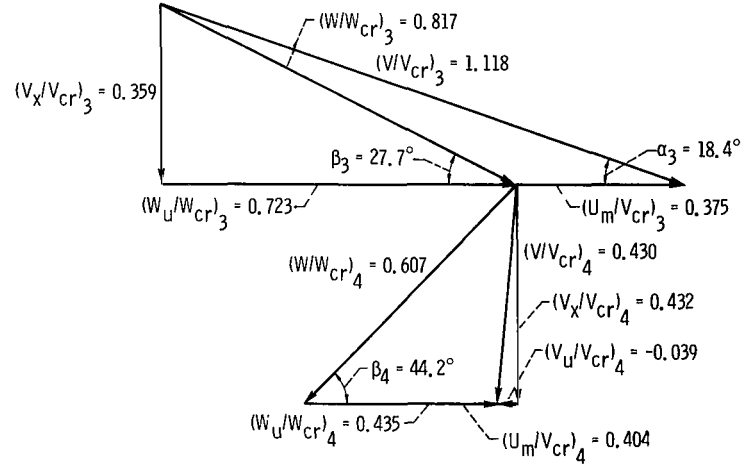

(d) Reynolds number, 187 730; inlet total pressure, 35.26 psia (24.31 N/cm^2).

Figure 11. - Free-stream velocity diagrams at blade-jet speed ratio of 0.32. Turbine overall static- to static-pressure ratio, P_1/P_5, 2.5.

The stator-outlet flow angle α_3 and the rotor-outlet relative flow angle β_4 are both close to the design values of 18.66° and 39.24°, except at the lowest Reynolds number of 4940. The β_4 value of 53.0° at this Reynolds number indicates flow separation of 14° at the rotor outlet. The reference turbine showed stator-outlet flow separation at Reynolds numbers below 14 000, and considerable rotor-outlet flow separation at all Reynolds numbers, which probably contributed to the lower efficiency level than that obtained in the subject investigation.

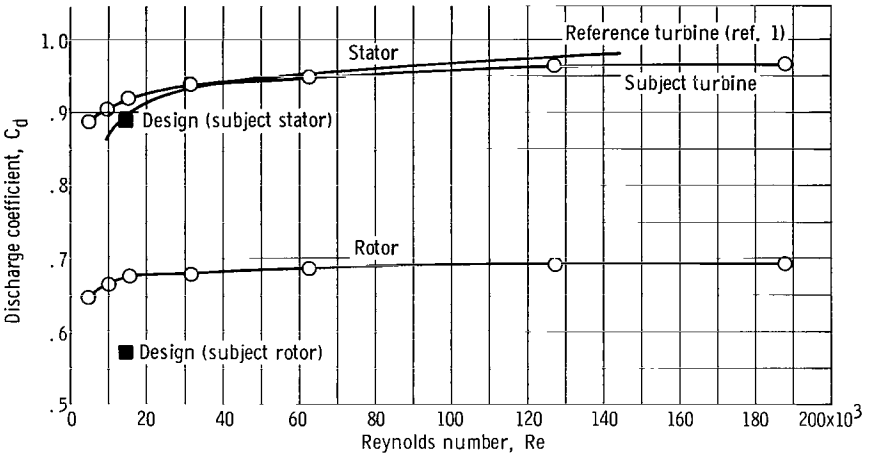

Figure 12. - Variation of stator and rotor discharge coefficients with Reynolds number. Subject-rotor overall static- to static-pressure ratio, p_1/p_5, 2.5; blade-jet speed ratio, 0.32.

Figure 12 shows the effect of Reynolds number on the subject-turbine and reference-turbine stator discharge coefficients C_d and on the subject-turbine rotor discharge coefficient. Through a Reynolds number range of 9400 to 144 000, the subject-turbine stator discharge coefficient varied from 0.90 to 0.965 compared with values of 0.86 to 0.98 for the reference turbine. At the design Reynolds number of 14 900, the subject-stator actual and design discharge coefficient values are 0.917 and 0.888, respectively. At a Reynolds number of 9400, the stator discharge coefficient for the subject turbine is four points higher than for the reference turbine, while at 144 000 it is one point lower. The low discharge coefficients shown for the reference turbine at low Reynolds numbers may be caused by the stator-exit flow separation which occurred at Reynolds numbers below 14 000.

The subject-turbine rotor discharge coefficient increased from 0.646 to 0.685 between Reynolds numbers of 4900 and 62 000. Above 62 000, the coefficient is nearly constant. At design Reynolds number, the discharge coefficient of 0.676 is 18.4 percent greater than the design value of 0.571.

Figure 13 shows the effect of Reynolds number on computed rotor reaction R. The low rotor losses, discussed above and in the section Velocity diagram calculation results

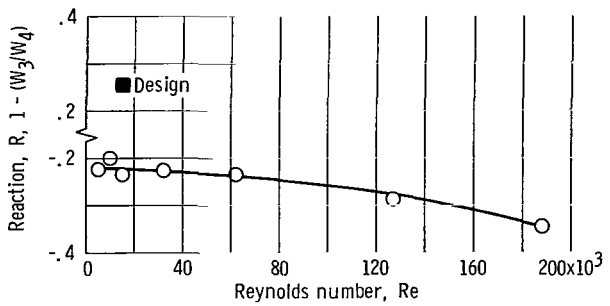

Figure 13. - Effect of Reynolds number on reaction across rotor. Blade-jet speed ratio, 0.32; turbine overall static- to static-pressure ratio, p_1/p_5, 2.5.

(p. 13), caused high stator discharge velocities. These high velocities resulted in negative reaction across the rotor at all Reynolds numbers. As Reynolds number increased from 4900 to 188 000, the rotor reaction decreased from -0.21 to -0.35. Design reaction was 0.257, while actual reaction at design inlet total pressure was -0.21. Although design reaction across the rotor was not attained and even though stator-exit velocity was greater than design, the turbine yielded higher-than-design efficiency.

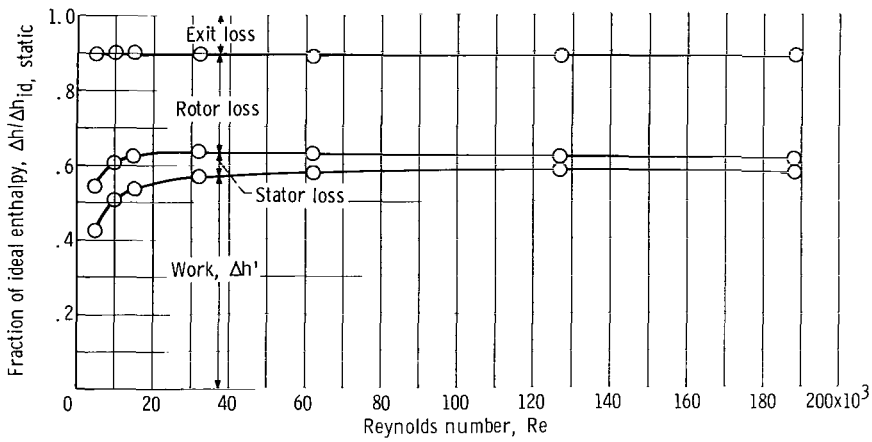

Figure 14. - Variation of energy distribution with Reynolds number. Turbine overall static- to static-pressure ratio, p_1/p_5, 2.5; blade-jet speed ratio, 0.32.

Figure 14 shows the variation with Reynolds number of energy distribution corresponding to the calculated velocity diagrams. Work and losses are expressed as fractions of ideal enthalpy based on exit-static- to inlet-total-pressure ratio. The stator loss decreased with increasing Reynolds number throughout the entire range of 4900 to 188 000. The rotor loss decreased between Reynolds numbers of 4900 and 15 000 and then remained approximately constant. The exit loss was almost constant at all Reynolds numbers. The following table compares the energy distribution for the extreme Reynolds numbers investigated (4900 and 188 000) in fractions of ideal enthalpy based on exit-static - to inlet-total-pressure ratio.

Reynolds number	Work	Stator loss	Rotor loss	Exit loss
4 900	0.423	0.121	0.349	0.108
188 000	.578	.034	.275	.113

SUMMARY OF RESULTS

A 4-inch- (10.16-cm-) mean-diameter turbine was tested in air over a range of inlet total pressures from 1.0 to 35.0 psia (0.69 to 24.13 N/cm^2), which corresponds to a Reynolds number range of 4900 to 188 000. Results were compared to those of a reference 4-inch- (10.16-cm-) mean-diameter turbine with higher peak suction surface velocities for rotor and stator and with higher rotor surface diffusion. The results are summarized as follows:

1. The turbine had higher peak static efficiencies than the reference turbine at all Reynolds numbers. Over a Reynolds number range from 9400 to 144 000, the subject-turbine peak efficiencies increased from 0.53 to 0.63 compared with corresponding values of 0.26 and 0.56 for the reference turbine. The improved efficiency of the subject turbine results from lower rotor losses than those of the reference turbine.

2. The flow separation which occurred at the stator and rotor outlets of the reference turbine was absent in the subject turbine except for the lowest Reynolds number of 4940 where a 14° deviation from design relative flow angle occurred at the rotor outlet.

3. Peak static efficiency for the subject turbine increased from 0.40 to 0.63, as the Reynolds number increased from 4900 to 127 000, and remained constant above this value.

4. At approximately design operating conditions, the rotor discharge coefficient was 18.4 percent greater than design. The low rotor losses caused overexpansion of the stator and resulted in negative values of rotor reaction ranging from -0.21 at the lowest Reynolds number of 4900 to -0.35 at 188 000. The design rotor reaction is 0.257.

5. At a blade-jet speed ratio of 0.32 and a turbine overall static- to static-pressure ratio of 2.5, losses varied with Reynolds number in the following manner: Stator losses, expressed as a fraction of ideal enthalpy, decreased from 0.121 to 0.034 over a Reynolds number range of 4900 to 188 000. Rotor losses decreased from 0.349 to 0.275, with almost all the decrease occurring below a Reynolds number of 15 000. Rotor-exit losses were practically constant at all Reynolds numbers.

Lewis Research Center,
National Aeronautics and Space Administration,
Cleveland, Ohio, September 19, 1967,
128-31-02-25-22.

APPENDIX A

SYMBOLS

C_d	discharge coefficient, ratio of measured weight flow to ideal weight flow based on inlet-total to exit-static pressure for stator and on relative inlet-total to exit-static pressure for rotor
D_p	pressure surface diffusion parameter, $1 - (W_{p,min}/W_i)$
D_s	suction surface diffusion parameter, $1 - (W_o/W_{s,max})$
D_t	$D_p + D_s$
h'	specific work output, Btu/lb; joules/g
J	mechanical equivalent of heat, 778 ft-lb/Btu
p	absolute pressure, psia; N/cm^2
R	rotor reaction, $1 - (W_3/W_4)$
Re	Reynolds number, $w/\mu_1 r$
r	rotor mean radius, ft; m
U	blade velocity, ft/sec; m/sec
V	absolute gas velocity, ft/sec; m/sec
V^*_{cr}	critical velocity at U.S. standard atmosphere sea-level conditions, 1019 ft/sec; 310.6 m/sec
W	relative gas velocity, ft/sec; m/sec
w	weight flow, lb/sec; kg/sec
α	absolute gas flow angle measured from tangential direction, deg
β	relative gas flow angle into or out of rotor measured from tangential direction, deg
γ	ratio of specific heats
δ	ratio of inlet-total pressure to U.S. standard atmosphere sea-level pressure, p'_2/p^*
η_s	static efficiency, ratio of actual specific work output to ideal specific work output based on ratio of exit-static to inlet-total pressure, p_4/p'_2
η_t	total efficiency, ratio of actual specific work output to ideal specific work output based on ratio of exit-total to inlet-total pressure, p'_4/p'_2

θ_{cr} squared ratio of critical velocity at turbine inlet to critical velocity at U. S. standard atmosphere sea-level temperature, $(V_{cr,1}/V^*_{cr})^2$

λ speed-work parameter, $U_m/\Delta V_u$, $2V^2/\eta_s$

μ viscosity, lb/(sec)(ft); N-sec/m^2

ν blade-jet speed ratio, $U_m/\sqrt{2gJ\ \Delta h_{id}}$

ρ gas density, lb/ft^3; kg/m^3

τ torque parameter, $\Delta V_u/\sqrt{gJ\ \Delta h_{id}}$

Subscripts:

cr conditions at Mach 1

i inlet of rotor

id ideal, based on total- to static-pressure ratio

m mean radius

max maximum

min minimum

o outlet of rotor blade row

p pressure surface

s suction surface

t total

u tangential direction

x axial direction

1 station at turbine-inlet collector

2 station at stator inlet

3 station between stator and rotor

4 station downstream from rotor

5 station at turbine-exit collector

Superscripts:

(') absolute total state

('') relative total state

(*) U. S. standard conditions (temperature, 518.7^o R (288.15^o K); pressure, 14.70 psia (10.14 N/cm^2)

APPENDIX B

VELOCITY DIAGRAM CALCULATION METHOD

Free-stream velocity diagrams were obtained from experimental data by the following general procedure.

Stator-Exit Diagrams

The stator discharge total pressure p'_3 was obtained by the method of reference 1 wherein the stator discharge coefficient C_d is used as the total-pressure loss coefficient. The absolute velocity ratio $(V/V_{cr})_3$ was computed from this total pressure and the measured static pressure p_3. The axial velocity ratio $(V_x/V_{cr})_3$ was obtained from the measured weight flow and the stator annulus area. Relative total temperature T''_3 was obtained from the equation

$$T''_3 = T'_3\left\{1 - \frac{\gamma - 1}{\gamma + 1}\left(\frac{U_m}{V_{cr}}\right)_3\left[2\left(\frac{V_u}{V_{cr}}\right)_3 - \frac{U_m}{(V_{cr})_3}\right]\right\}$$

The relative tangential velocity ratio $(W_u/W_{cr})_3$ was computed from $(V_u/V_{cr})_3$ and $(U_m/V_{cr})_3$.

Rotor-Outlet Diagrams

The turbine-exit total temperature T'_4 was obtained from the specific work output $\Delta h'$. The change in tangential velocity ΔV_u was computed from $\Delta h'$ and the mean-suction blade velocity U_m. The tangential velocity ratio $(V_u/V_{cr})_4$ and the relative tangential velocity ratio $(W_u/W_{cr})_4$ were obtained from ΔV_u and the rotor-inlet velocity diagram. The product of the rotor-outlet axial velocity and density $(\rho V_x)_4$ was obtained from the rotor annulus area and the measured weight flow. An iteration was then used to obtain a complete rotor-exit velocity diagram consistent with the preceding information.

REFERENCES

1. Wong, Robert Y.; and Nusbaum, William J.: Air-Performance Evaluation of a 4.0-Inch-Mean-Diameter Single-Stage Turbine at Various Inlet Pressures from 0.14 to 1.88 Atmospheres and Corresponding Reynolds Numbers from 2500 to 50,000. NASA TN D-1315, 1962.

2. Stewart, Warner L.; Wong, Robert Y.; and Evans, David G.: Design and Experimental Investigation of Transonic Turbine with Slight Negative Reaction Across Rotor Hub. NACA RM E53L29a, 1954.

3. Stewart, Warner L.; Whitney, Warren J.; and Wong, Robert Y.: A Study of Boundary-Layer Characteristics of Turbomachine Blade Rows and Their Relation to Over-All Blade Loss. J. Basic Eng., vol. 82, no. 3, Sept. 1960, pp. 588-592.

4. Stewart, Warner L.: A Study of Axial-Flow Turbine Efficiency Characteristics in Terms of Velocity Diagram Parameters. Paper No. 61-WA-37, ASME, 1961.

TABLE I. - STATOR BLADE COORDINATES

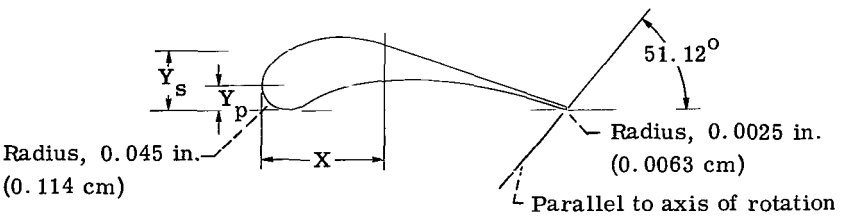

X		Y_p		Y_s	
in.	cm	in.	cm	in.	cm
0	0	0.0450	0.1143	0.0450	0.1143
.0200	.0508	.0076	.0193	.0914	.2322
.0400	.1016	------	------	.1116	.2835
.0600	.1524	.0028	.0071	.1240	.3150
.0800	.2032	.0154	.0391	.1316	.3343
.1000	.2540	.0292	.0742	.1354	.3439
.1200	.3048	.0412	.1046	.1364	.3465
.1400	.3556	.0506	.1285	.1352	.3434
.1600	.4064	.0576	.1463	.1324	.3363
.1800	.4572	.0630	.1600	.1278	.3246
.2000	.5080	.0668	.1697	.1224	.3109
.2200	.5588	.0688	.1748	.1164	.2957
.2400	.6096	.0698	.1773		
.2600	.6604	.0698	.1773		
.2800	.7112	.0682	.1732		
.3000	.7620	.0662	.1681		
.3200	.8128	.0632	.1605		
.3400	.8636	.0594	.1509		
.3600	.9144	.0552	.1402		
.3800	.9652	.0502	.1275		
.4000	1.0160	.0448	.1138		
.4200	1.0668	.0394	.1001		
.4400	1.1176	.0334	.0849		
.4600	1.1684	.0268	.0681		
.4800	1.2192	.0204	.0518		
.5000	1.2700	.0136	.0345		
.5200	1.3208	.0070	.0178	.0120	.0305
.5430	1.3792	.0025	.0063	.0025	.0064

TABLE II. - ROTOR BLADE COORDINATES

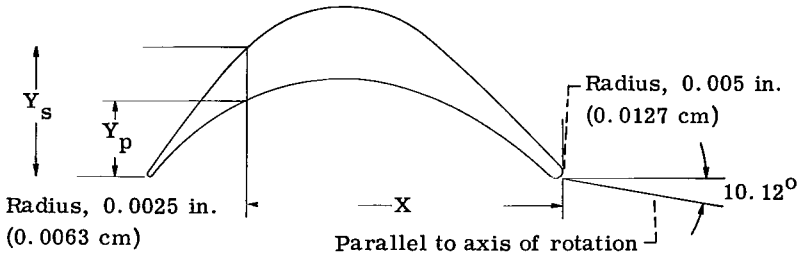

X		Y_p		Y_s	
in.	cm	in.	cm	in.	cm
0	0	0.0050	0.0127	0.0050	0.0127
.0100	.0254	.0034	.0086	.0230	.0584
.0200	.0508	.0184	.0467	.0398	.1011
.0300	.0762	.0302	.0767	.0567	.1440
.0400	.1016	.0397	.1008	.0721	.1831
.0500	.1270	.0470	.1194	.0825	.2096
.0600	.1524	.0531	.1349	.0899	.2283
.0700	.1778	.0577	.1466	.0947	.2405
.0800	.2032	.0612	.1554	.0978	.2484
.0900	.2286	.0639	.1623	.0994	.2525
.1000	.2540	.0657	.1669	.0995	.2527
.1100	.2794	.0666	.1692	.0985	.2502
.1200	.3048	.0668	.1697	.0961	.2441
.1300	.3302	.0660	.1676	.0924	.2347
.1400	.3556	.0644	.1636	.0877	.2228
.1500	.3810	.0619	.1572	.0819	.2080
.1600	.4064	.0585	.1486	.0755	.1918
.1700	.4318	.0542	.1377	.0683	.1735
.1800	.4572	.0492	.1250	.0609	.1547
.1900	.4826	.0435	.1105	.0533	.1354
.2000	.5080	.0372	.0945	.0456	.1158
.2100	.5334	.0303	.0770	.0378	.0960
.2200	.5588	.0232	.0589	.0300	.0762
.2300	.5842	.0157	.0399	.0222	.0564
.2400	.6096	.0081	.0206	.0144	.0366
.2500	.6350	.0004	.0010	.0066	.0168
.2537	.6444	.0025	.0063	.0025	.0063

"The aeronautical and space activities of the United States shall be conducted so as to contribute . . . to the expansion of human knowledge of phenomena in the atmosphere and space. The Administration shall provide for the widest practicable and appropriate dissemination of information concerning its activities and the results thereof."

—NATIONAL AERONAUTICS AND SPACE ACT OF 1958

NASA SCIENTIFIC AND TECHNICAL PUBLICATIONS

TECHNICAL REPORTS: Scientific and technical information considered important, complete, and a lasting contribution to existing knowledge.

TECHNICAL NOTES: Information less broad in scope but nevertheless of importance as a contribution to existing knowledge.

TECHNICAL MEMORANDUMS: Information receiving limited distribution because of preliminary data, security classification, or other reasons.

CONTRACTOR REPORTS: Scientific and technical information generated under a NASA contract or grant and considered an important contribution to existing knowledge.

TECHNICAL TRANSLATIONS: Information published in a foreign language considered to merit NASA distribution in English.

SPECIAL PUBLICATIONS: Information derived from or of value to NASA activities. Publications include conference proceedings, monographs, data compilations, handbooks, sourcebooks, and special bibliographies.

TECHNOLOGY UTILIZATION PUBLICATIONS: Information on technology used by NASA that may be of particular interest in commercial and other non-aerospace applications. Publications include Tech Briefs, Technology Utilization Reports and Notes, and Technology Surveys.

Details on the availability of these publications may be obtained from:

SCIENTIFIC AND TECHNICAL INFORMATION DIVISION

NATIONAL AERONAUTICS AND SPACE ADMINISTRATION

Washington, D.C. 20546